Reversible Pair Substitution in CIDNP: The Radical Cation of Methionine

Martin Goez*,† and Jaroslaw Rozwadowski‡

Fachbereich Chemie, Martin-Luther-Universität Halle-Wittenberg, Kurt-Mothes-Strasse 2, D-06120 Halle/Saale, Germany, and Faculty of Chemistry, Adam Mickiewicz University Poznan, Grunwaldzka 6, PL 60-780 Poznan, Poland

Received: April 8, 1998; In Final Form: July 6, 1998

CIDNP spectroscopy (measurements of chemically induced dynamic nuclear polarization) is applied to the photoreaction of methionine with 4-carboxybenzophenone in D_2O at varying pH (5.8, ..., 12.2). By using the polarization pattern of the regenerated amino acid, the interconversion of the different forms of the methionine radical cation (open-chain protonated, open-chain deprotonated, and cyclic, with a two-center-three-electron bond between sulfur and nitrogen) is studied. The change of the CIDNP pattern with pH is not due to a protonation preequilibrium but is a rate phenomenon. To extract rate constants from the pH dependence of the polarization pattern, the theory of pair substitution in CIDNP is extended to cover reversible reactions with arbitrary equilibrium constants. This problem is treated with the Freed−Pedersen reencounter formalism. Spin dynamics and radical pair dynamics are separated by the assumption of an exchange volume. General expressions for the spin-dependent recombination probabilities in the strong-exchange limit are derived, as well as solutions for a specific diffusional model (Noyes' model); the latter are used to fit the experimental data. It is shown that neither the assumption of slow (on the CIDNP time scale) protonation/deprotonation nor that of pH-independent reaction rates can explain the observed effects. When the rate of the backward reaction is proportional to $[H^+]$, which follows from the assumption that cyclization of the deprotonated open-chain radical cation is fast on the CIDNP time scale, a very good fit can be reached. The p*K* value for deprotonation concomitant with cyclization is found to be 8.15. By comparison with model compounds it is estimated that the equilibrium constant for cyclization of the deprotonated radical cation is about 2.5.

Introduction

Of all the methods for probing structure and dynamics of transient radicals and radical ions in solution, magnetic resonance techniques yield the most direct information because they are sensitive to the distribution of the unpaired spin density. CIDNP[1] (chemically induced dynamic nuclear polarization) spectroscopy is a variant of magnetic resonance that is particularly well suited for the investigation of complex reaction mechanisms involving radical pairs as intermediates. The observables in a CIDNP experiment are nonequilibrium populations (polarizations) of the nuclear spin states in the diamagnetic reaction products, which manifest themselves as anomalous line intensities in NMR spectra recorded during the reaction or immediately afterwards. CIDNP arises through the interplay of what has been termed spin dynamics and radical pair dynamics. Spin dynamics denotes the evolution of the electron spin state of the pairs by coherent precession under the influence of magnetic interactions; through the hyperfine interaction, the rate of this evolution depends on the nuclear spin states of the radicals. Radical pair dynamics comprises diffusion and electron-spin selective as well as nonselective chemical reactivity of the radicals. Operating in conjunction, spin dynamics and radical pair dynamics effect a sorting of the nuclear spins between different types of products.

This intricate mechanism has several unusual features that can be put to good use. For one thing, the relative polarization intensities of the different protons or other nuclei in the diamagnetic products (the "polarization pattern")[2] are directly related to and quite frequently identical with the corresponding relative hyperfine coupling constants in the paramagnetic intermediates. The polarization pattern, therefore, represents an uncalibrated EPR spectrum of the radicals, with the unique advantage of often revealing immediately which hyperfine coupling constant belongs to which nucleus.[3a] What is more, the polarization pattern can be regarded as a frozen signature of the intermediates because the time frame for CIDNP generation is fixed by the life of the pairs (0.1−10 ns), but once generated the polarizations persist in the diamagnetic products for the spin-lattice relaxation time T_1 (typically 1−10 s for protons). CIDNP thus responds to faster processes than does EPR, and CIDNP spectroscopy has frequently been used[3] to identify radicals and radical ions that escape detection by EPR. As a third consequence, which is of central importance for the present work, the polarizations are sensitive to transformations of the radical pairs into other radical pairs ("pair substitution") when these transformations occur on the time scale of the CIDNP effect.[4] The evolution of the electron spin state provides an inherent clock against which the reaction rates can be measured.

The radical cation of methionine,[5] which is an intermediate of potential significance for long-range electron transfer across cell membranes[6a] or oxidative damage of cell components,[6b] is an interesting candidate for CIDNP studies. On the one hand, it is too short-lived in liquid solution to allow observation by EPR but can be easily detected and characterized by CIDNP.[5e] On the other hand, it can exist in quite different structures (see Chart 1), which is reflected by the polarization patterns.[5e] It is

* Author to whom correspondence should be addressed.
† Fachbereich Chemie.
‡ Faculty of Chemistry.

S1089-5639(98)01791-5 CCC: $15.00
Published on Web 09/17/1998

CHART 1

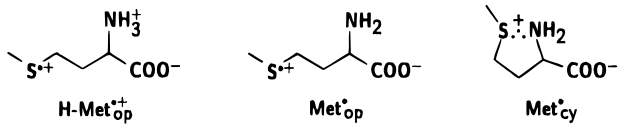

established that its primary form in sensitized photooxidations is an open-chain sulfur-centered[5e] radical cation H-Met$^{\bullet+}_{op}$ (or its *N*-deprotonated form Met$^{\bullet}_{op}$, which is still a radical cation *locally*).[7] The open-chain species can undergo cyclization to give a five-membered ring Met$^{\bullet}_{cy}$ with a two-center-three-electron bond between sulfur and nitrogen.[5] This two-center-three-electron bond cannot be formed when the amino function is protonated because then it cannot act as an electron donor. As a result, different polarization patterns are observed at low and high pH.[5e]

In the present work, we have quantitatively explored the pH dependence of the polarization pattern. As we will show, this dependence cannot be explained by a protonation preequilibrium alone (i.e., by the protonation equilibrium of the starting amino acid); reversible protonation of the radical cation contributes significantly to and takes place within the kinetic window of the CIDNP effect. The rate of deprotonation and the pK_a value of the radical cation are obtained from a fit to a theoretical model. To this end, the theory of pair substitution in CIDNP is extended to cover reversible transformations of two radical pairs RP 1 ⇌ RP 2 with arbitrary equilibrium constants, which contains previously given solutions[4] for pair substitution as special cases.

Results and Discussion

CIDNP Experiments. CIDNP measurements in the system methionine/4-carboxybenzophenone were performed between pH 5.8 and 12.2. Throughout this pH range, the sensitizer is present in its anionic form[8] while the amino acid is present in its zwitterionic form H-Met below pK_{a2} (9.66, see below) and in its deprotonated form Met$^-$ above pK_{a2}. To simplify the nomenclature, we omit the charge on the carboxy group of the sensitizer; thus, we denote the ketone as CB and its radical anion as CB$^{\bullet-}$. Figure 1 shows representative CIDNP spectra at different pH in this system.

The protons of the starting amino acid are polarized in absorption because the precursor multiplicity is triplet, the educts are regenerated by back electron transfer of singlet radical pairs, the *g* values of all the methionine-derived radicals in Chart 1 (as well as of the hydroxy sulfuranyl species)[7] are larger than the *g* value of CB$^{\bullet-}$, and the proton hyperfine coupling constants in any of them are positive.[5e,9,10] In consequence of the spin sorting mechanism of CIDNP, the protons of the other products (i.e., of those due to radicals escaping from triplet pairs) are emissively polarized. However, these signals will not be discussed here because they have no bearing on the question as to the structure of the methionine radical cation.[5e]

Decarboxylation of the methionine radical cations ($\tau_{1/2} \approx 220$ ns)[5a] to give α-aminoalkyl radicals is fast compared to the life of the free radicals but slow compared to that of the spin-correlated radical pairs. Therefore, pairs formed by chance encounters of free radicals (*F* pairs) only play a role for the polarizations of secondary products but do not lead to polarizations in the regenerated starting amino acid; on the other hand, the educt polarizations, which stem from pairs with triplet precursors, are not influenced by the decarboxylation.

The β and δ protons of the amino acid (for the notation, see the formula at the top of the figure) fall into a crowded spectral region around 2.0 ppm, where partial cancelation by a large emission signal occurs, so they are suited less well for quantitative evaluation; besides, H$^{\beta}$ is not appreciably polarized. Hence, the spectral range of Figure 1 has been chosen such as to include only H$^{\alpha}$ and H$^{\gamma}$. The γ protons (i.e., those at a carbon adjacent to sulfur) are seen to be polarized throughout the whole pH range while the α proton (i.e., that at the carbon attached to nitrogen) is only polarized at high pH. This reflects the fact that all forms of the methionine radical cation (Chart 1) possess a substantial spin density on sulfur, but only in the cyclic radical cation Met$^{\bullet}_{cy}$ is there a nonnegligible spin density on nitrogen.[5e]

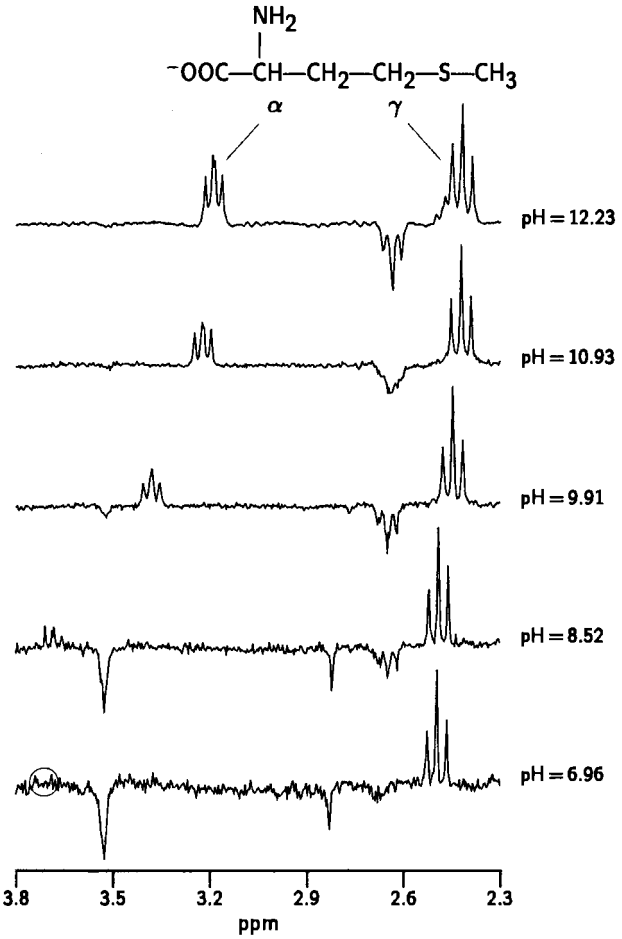

Figure 1. Background-free ^{1}H-CIDNP spectra (250 MHz) observed during the photoreactions of 4-carboxybenzophenone with methionine in D_2O at different pH values (given at the right). Only the relevant spectral region is shown. The methionine resonances of interest are polarized in absorption, the signals of H$^{\alpha}$ appearing in the left part of the spectra (between 3.18 and 3.70 ppm, depending on pH) and the signals of H$^{\gamma}$ at the right (between 2.42 and 2.49 ppm). At pH 6.96, the signal of H$^{\alpha}$ is extremely weak. Its position is indicated by the circle. The formula of methionine in its deprotonated form Met$^-$ is displayed at the top. The spectra were normalized with respect to the triplet of H$^{\gamma}$.

Because in the open-chain structures there is no interaction between the nitrogen and sulfur termini, protonation of the amino function cannot influence the spin density distribution in the thioether group significantly. Hence, the hyperfine coupling constant of H$^{\gamma}$ must be essentially the same in H-Met$^{\bullet+}_{op}$ and Met$^{\bullet}_{op}$ (and also similar in the hydroxy sulfuranyl radical),[7,11] and a distinction between these species by CIDNP is impossible. Of the three protonation/cyclization equilibria of the methionine radical cation shown in Chart 2, at best only two are thus accessible to CIDNP experiments. However, the

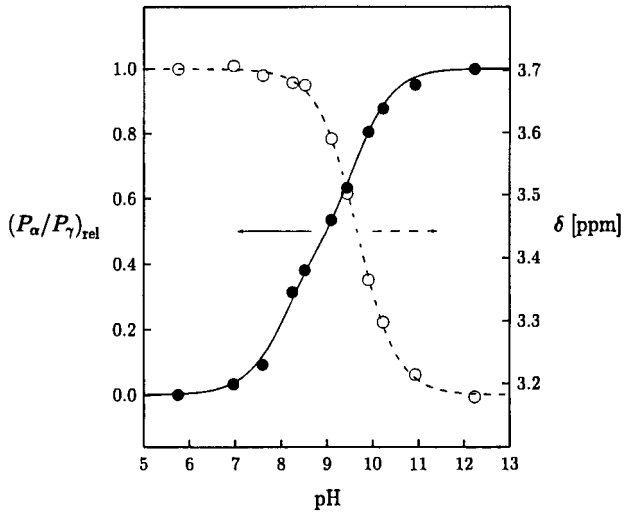

Figure 2. Quantitative results of a series of pH-dependent measurements as shown in Figure 1. Filled circles, polarizations ratios $(P_\alpha/P_\gamma)_{rel}$ of the α and γ protons of methionine normalized to a maximum value of 1.0. The solid line is a fit curve based on a model of reversible pair substitution (see below). Open circles, chemical shifts of H^α. The broken line is a fit with eq 2. The arrows indicate the pertaining vertical scale of each curve.

CHART 2

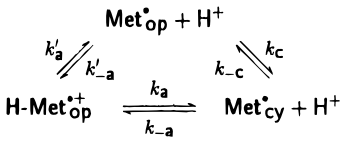

three equilibrium constants are of course related by

$$K_a = K'_a K_c \tag{1}$$

Another conspicuous phenomenon in Figure 1 besides the change of the CIDNP intensities is the pronounced high-field shift of the signal of H^α with rising pH. This is due to deprotonation of the amino function in the educt, the α proton being more deshielded in H-Met than in Met^-. The influence of pH on the polarization pattern and on the resonance frequency of H^α is displayed quantitatively in Figure 2. Absolute CIDNP measurements are often unreliable, above all because the polarization intensity is directly proportional to the number of radical pairs formed, which in turn is certainly pH dependent for the system under study—compare the different signal-to-noise ratios in the spectra of Figure 1, which were all recorded under identical conditions except for the pH value. Using relative CIDNP intensities instead is much less prone to errors. Therefore, the ratio of the polarizations of H^α and H^γ has been plotted in Figure 2.

As shown in the figure, the chemical shift can be excellently fitted with a function

$$\delta = \frac{10^{-\mathrm{pH}}\delta_p + 10^{-\mathrm{p}K_{a2}}\delta_{up}}{10^{-\mathrm{pH}} + 10^{-\mathrm{p}K_{a2}}} \tag{2}$$

where δ_p and δ_{up} are the chemical shifts of pure H-Met and pure Met^-, respectively. Equation 2 is simply a titration curve, which is characterized by pK_{a2} of the amino acid. From the best fit, pK_{a2} is found to be 9.66, 0.39 units higher than the literature[12] value. The reason for this discrepancy is that our experiments are carried out in D_2O. Almost the same difference between pK_{a2} for protonation and for deuteration is found in the case of *S*-(methyl)cysteine.[3b]

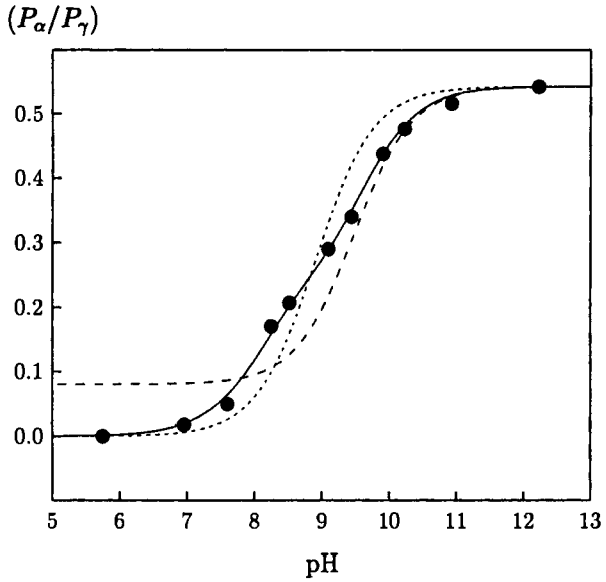

Figure 3. Best fits to the pH-dependent experimental polarization ratios P_α/P_γ (filled circles) of the α and γ protons of methionine for different models. Short dashes, protonation preequilibrium; long dashes, reversible pair substitution RP 1 ⇌ RP 2 with pH-independent rate constants; solid line, reversible pair substitution when the rate constant of the back reaction is proportional to $[H^+]$. For further explanation, see text.

The pH dependence of the polarization ratio also has a sigmaoidal shape and might thus at first glance be regarded as a titration curve as well, though this is not corroborated by the fit results (compare below, Figure 3). In any case, however, it is immediately obvious that the associated pK_a value would differ noticeably from pK_{a2} of the amino acid. As a corollary, the pH dependence of the CIDNP pattern cannot simply be due to a superposition of polarizations from two noninterconverting radical pairs, one formed from H-Met and the other from Met^-. There must be a contribution from proton-transfer processes at the radical pair stage, and these processes must also be accompanied by changes of the spin density distribution because otherwise the polarization pattern could not change. Hence, the observed effects must be related to the equilibria shown in Chart 2. Evidently, these equilibria are at least partly established within the kinetic window of CIDNP, so for their theoretical description and for extraction of parameters from the experimental data a theory of reversible pair substitution is needed.

Density Matrix Treatment of Pair Substitution. Pair substitution in CIDNP has been addressed in the literature for one or more successive irreversible transformations RP1 → RP2 (→ ...),[4] and for the special case of an equilibrium between RP 1 and RP 2 with equilibrium constant $K = 1$.[4a] In the following, we consider a reaction RP 1 ⇌ RP 2 with arbitrary equilibrium constant.

The problem is treated with the Freed−Pedersen reencounter formalism[13] because this yields a particularly transparent physical description. Spin dynamics and radical pair dynamics are separated by using the approximation of an exchange region.[13a] Solutions of the equations of motion for the density vector are derived first, and then assembled with the dynamic probability function of reencounter. After obtaining general expressions that are independent of a diffusional model, a solution for the Noyes model[17] is given, which is finally used to fit the experimental data.

Spin Dynamics. As usual in high-field radical pair theory, intersystem crossing between $|S\rangle$ and $|T_0\rangle$ is considered only,

and electron spin relaxation is neglected. Under these conditions, the density matrix of an ensemble of radical pairs can be written as a vector of four real components, which are physically meaningful quantities,[14]

$$\begin{pmatrix} \rho_{SS} + \rho_{T_0T_0} \\ \rho_{SS} - \rho_{T_0T_0} \\ i(\rho_{T_0S} - \rho_{ST_0}) \\ \rho_{ST_0} + \rho_{T_0S} \end{pmatrix} = \begin{pmatrix} \text{total population} \\ \text{population difference} \\ \text{phase correlation} \\ \text{electron spin polarization} \end{pmatrix}$$

Thus, a density vector of dimension eight fully describes the ensemble of two interconverting radical pairs RP 1 and RP 2.

As long as the chemical system is closed (i.e., in the absence of geminate recombination of the pairs and escape from the cage) the total populations $\vec{\rho}_{tot}$,

$$\vec{\rho}_{tot} = \begin{pmatrix} (\rho_{SS} + \rho_{T_0T_0})_{RP\,1} \\ (\rho_{SS} + \rho_{T_0T_0})_{RP2} \end{pmatrix}$$

are decoupled from the other components. The time-dependence of $\vec{\rho}_{tot}$ is given by

$$\frac{d\,\vec{\rho}_{tot}}{dt} = \begin{pmatrix} -k_{for} + k_{bck} \\ +k_{for} - k_{bck} \end{pmatrix} \vec{\rho}_{tot} \qquad (3)$$

where k_{for} is the first-order rate constant of the reaction RP 1 → RP 2 and k_{bck} that of the reverse process. The solution of eq 3, which is simply the chemical rate law for the concentrations of RP 1 and RP 2, is

$$\vec{\rho}_{tot}(t) = \begin{pmatrix} F(k_{for}, k_{bck}) & 1 - F(k_{bck}, k_{for}) \\ 1 - F(k_{for}, k_{bck}) & F(k_{bck}, k_{for}) \end{pmatrix} \vec{\rho}_{tot}(0) \qquad (4)$$

with the initial condition $\vec{\rho}_{tot}(0)$ and the abbreviation

$$F(\kappa_1, \kappa_2) = \frac{\kappa_1 \exp[-(\kappa_1 + \kappa_2)t] + \kappa_2}{\kappa_1 + \kappa_2} \qquad (5)$$

This representation of the solution, where the function F is computed once with the arguments k_{for} and k_{bck}, in that order, and once with k_{for} and k_{bck} interchanged, has been chosen to emphasize the symmetry properties; it is also practical for numerical calculations.

The remaining six components of the density vector fall into two sets of three, one set for RP 1 and one for RP 2. By the chemical transformation each component (e.g., the population difference) of the first set "leaks" to the corresponding component of the second set and vice versa. Furthermore, the three components within each set j are mixed by the interplay of the exchange interaction J_j and the matrix element q_j of intersystem crossing driven by differential precession frequencies of the two radicals,[15]

$$q_j = \frac{1}{\hbar}[(g_{j1} - g_{j2})\beta B_0 + \sum_i a_{ji} m_{ji} - \sum_k a_{jk} m_{jk}], \quad j = 1, 2 \qquad (6)$$

In eq 6, g_{j1} and g_{j2} are the g values of radical 1 and radical 2 in pair j; a_{ji} and m_{ji} are the hyperfine coupling constant and z-spin quantum number of nucleus i in radical 1 of pair j, a_{jk}, and m_{jk} those of nucleus k in radical 2 of that pair.

Because of the strong distance dependence of J, the concept of an exchange region can be introduced.[13a] Within this region (i.e., for the short time before or after an encounter when the two radicals of a pair reside near one another) the spin Hamiltonian is completely dominated by J, which mixes phase correlation and electron spin polarization only. Outside this region (i.e., for the most part of a diffusional excursion), J is negligible compared to q, and the latter mixes phase correlation and population difference only. A vector $\vec{\rho}'$ of four components, therefore, completely describes the spin dynamics of the system during a diffusional excursion outside the exchange region. It is under these conditions that the nuclear spin polarizations arise.

In the absence of the chemical reaction RP 1 ⇌ RP 2, the evolution of $\vec{\rho}'$,

$$\vec{\rho}' = \begin{pmatrix} (\rho_{SS} - \rho_{T_0T_0})_{RP\,1} \\ i\,(\rho_{T_0S} - \rho_{ST_0})_{RP\,1} \\ (\rho_{SS} - \rho_{T_0T_0})_{RP\,2} \\ i\,(\rho_{T_0S} - \rho_{ST_0})_{RP\,2} \end{pmatrix}$$

can be regarded as two independent rotations, one in the subspace of RP 1 and one in that of RP 2. The interconversion of the pairs simply couples these rotations. Except for the absence of relaxation terms, the situation is completely analogous to that encountered in dynamic NMR spectroscopy of a spin-$^1/_2$ nucleus jumping reversibly between two sites 1 and 2, where it possesses different precession frequencies.

It is advantageous to express the system of four real differential equations for $\vec{\rho}'$ as a system of two complex differential equations by introducing the variables z_1 and z_2, one for each type of radical pair,

$$z_j = (\rho_{SS} - \rho_{T_0T_0})_{RP\,j} - (\rho_{T_0S} - \rho_{ST_0})_{RP\,j}, \quad j = 1, 2$$

where the real part is the population difference and the imaginary part the phase correlation. In this way, one gets

$$\begin{pmatrix} \dot{z}_1 \\ \dot{z}_2 \end{pmatrix} = \begin{pmatrix} -k_{for} + iq_1 & +k_{bck} \\ +k_{for} & -k_{bck} + iq_2 \end{pmatrix} \begin{pmatrix} z_1 \\ z_2 \end{pmatrix} \qquad (7)$$

The solution of eq 7 is

$$\vec{z}(t) = \frac{1}{w} \begin{pmatrix} \mu_+ \exp(\nu_+ t) - \mu_- \exp(\nu_- t) & k_{bck}[\exp(\nu_+ t) - \exp(\nu_- t)] \\ k_{for}[\exp(\nu_+ t) - \exp(\nu_- t)] & \mu_+ \exp(\nu_- t) - \mu_- \exp(\nu_+ t) \end{pmatrix} \vec{z}(0) \qquad (8)$$

with the abbreviations

$$w = \sqrt{[(k_{for} + k_{bck})^2 - (q_1 - q_2)^2] + 2i\,(k_{bck} - k_{for})\,(q_1 - q_2)} \qquad (9)$$

$$\mu_\pm = \{[(k_{bck} - k_{for}) + i\,(q_1 - q_2)] \pm w\}/2 \qquad (10)$$

$$\nu_\pm = [-(k_{for} + k_{bck}) + i\,(q_1 + q_2) \pm w\}/2 \qquad (11)$$

Simulations of diffusional trajectories[16] indicate that for realistic parameters practically complete randomization of phase correlation and electron spin polarization occurs within the exchange region before a reencounter (strong-exchange limit).[1b] Hence, for the present analysis the electron spin polarization may be completely disregarded, while the phase correlation can be taken to be zero at the start of a diffusional excursion and is only needed for the intermediate calculations because it is destroyed upon reencounter. The population differences $\vec{\rho}_{diff}$,

$$\vec{\rho}_{diff} = \begin{pmatrix} (\rho_{SS} - \rho_{T_0T_0})_{RP\,1} \\ (\rho_{SS} - \rho_{T_0T_0})_{RP\,2} \end{pmatrix}$$

are thus obtained from eq 8 by letting the components of $\vec{z}(0)$

to be real and taking the real part of $\vec{z}(t)$. The result can be written as

$$\vec{\rho}_{\mathrm{diff}}(t) = \begin{pmatrix} G\,(k_{\mathrm{for}}, k_{\mathrm{bck}}; q_1, q_2) & H\,(k_{\mathrm{for}}, k_{\mathrm{bck}}; q_{\mathrm{l}}, q_2) \\ H\,(k_{\mathrm{bck}}, k_{\mathrm{for}}; q_2, q_1) & G\,(k_{\mathrm{bck}}, k_{\mathrm{for}}; q_2, q_1) \end{pmatrix} \vec{\rho}_{\mathrm{diff}}(0) \tag{12}$$

where

$$\begin{aligned} G\,(\kappa_1, \kappa_2; \omega_1, \omega_2) = \\ {}^1/_2\{&\exp(-u_+t)\cos(v_+t)\,[1 + \alpha\,(\kappa_1, \kappa_2; \omega_1, \omega_2)] + \\ &\exp(-u_-t)\cos(v_-t)\,[1 - \alpha\,(\kappa_1, \kappa_2; \omega_1, \omega_2)] + \\ &[\exp(-u_+t)\sin(v_+t) - \exp(-u_-t)\sin(v_-t)] \times \\ &\beta(\kappa_1, \kappa_2; \omega_1, \omega_2)\} \end{aligned} \tag{13}$$

$$\begin{aligned} H\,(\kappa_1, \kappa_2; \omega_1, \omega_2) = \\ \frac{\kappa_2}{\mathrm{Re}^2\, w + \mathrm{Im}^2\, w}\{&[\exp(-u_-t)\cos(v_-t) - \\ &\exp(-u_+t)\cos(v_+t)]\,\mathrm{Re}\, w + [\exp(-u_+t)\sin(v_+t) - \\ &\exp(-u_-t)\sin(v_-t)]\,(-\mathrm{Im}\, w)\} \end{aligned} \tag{14}$$

$$\alpha(\kappa_1, \kappa_2; \omega_1, \omega_2) = \frac{(\kappa_1 - \kappa_2)\,\mathrm{Re}\, w + (\omega_1 - \omega_2)\,(-\mathrm{Im}\, w)}{\mathrm{Re}^2\, w + \mathrm{Im}^2\, w} \tag{15}$$

$$\beta(\kappa_1, \kappa_2; \omega_1, \omega_2) = \frac{(\omega_1 - \omega_2)\,\mathrm{Re}\, w - (\kappa_1 - \kappa_2)\,(-\mathrm{Im}\, w)}{\mathrm{Re}^2\, w + \mathrm{Im}^2\, w} \tag{16}$$

$$u_\pm = (k_{\mathrm{for}} + k_{\mathrm{bck}} \pm \mathrm{Re}\, w)/2 \tag{17}$$

$$v_\pm = [q_1 + q_2 \pm (-\mathrm{Im}\, w)]/2 \tag{18}$$

As in eq 4, the notation has been chosen to bring out the symmetry properties of the solutions, and to facilitate numerical calculations. Each function G and *H* must be computed twice, once with the variables in the "normal" order, and the second time with the two rate constants as well as the two matrix elements of intersystem crossing interchanged. It is seen that the coefficients α and β are antisymmetric with respect to interchange of the two radical pairs (i.e., they change sign upon the described permutation of arguments). The real and imaginary parts of the square root *w* (eq 9) are given by

$$\mathrm{Re}\, w = \sqrt{\frac{\sqrt{\lambda^2 + \xi^2} + \lambda}{2}} \tag{19}$$

$$-\mathrm{Im}\, w = -\mathrm{sign}\,\xi\sqrt{\frac{\sqrt{\lambda^2 + \xi^2} - \lambda}{2}} \tag{20}$$

with

$$\lambda = (k_{\mathrm{for}} + k_{\mathrm{bck}})^2 - (q_1 - q_2)^2$$

$$\xi = 2(k_{\mathrm{for}} - k_{\mathrm{bck}})\,(q_1 - q_2)$$

Re *w* and Im *w* are symmetric with respect to interchange of the two radical pairs, as are $u_\pm$ and $v_\pm$. In order for the terms $\exp(-u_-t)$ to be bounded, $(k_{\mathrm{for}} + k_{\mathrm{bck}} - \mathrm{Re}\, w)$ must not become negative. However, it can be shown that this condition is always fulfilled for positive values of k_{for} and k_{bck}.

In contrast to $\vec{\rho}_{\mathrm{tot}}$, where the equilibrium value remains as nonzero limit at long times, the elements of $\vec{\rho}_{\mathrm{diff}}$ decay to zero because the (uncorrelated) jumping between RP 1 and RP 2 gradually effects complete phase randomization.

Special cases that were already treated in the literature, such as an equilibrium constant of unity[4a] or a one-sided reaction[4c], can be obtained from the solution presented here by letting $k_{\mathrm{for}} = k_{\mathrm{bck}}$ or $k_{\mathrm{bck}} = 0$, respectively.

Combining Spin Dynamics and Radical Pair Dynamics. To describe electron-spin selective geminate reactions of the radical pairs upon reencounter, it is necessary to transform from the coupled representations $\vec{\rho}_{\mathrm{tot}}$ and $\vec{\rho}_{\mathrm{diff}}$ to the representation $\vec{\rho}$ by the individual density matrix elements,

$$\vec{\rho} = \begin{pmatrix} (\rho_{\mathrm{SS}})_{\mathrm{RP\ 1}} \\ (\rho_{\mathrm{T_0T_0}})_{\mathrm{RP\ 1}} \\ (\rho_{\mathrm{SS}})_{\mathrm{RP\ 2}} \\ (\rho_{\mathrm{T_0T_0}})_{\mathrm{RP\ 2}} \end{pmatrix}$$

Let diffusional excursions of an ensemble of radical pairs (consisting of RP 1 and RP 2) start at an interradical distance r_0 at time $t = 0$ and terminate by a reencounter at distance *d*. Denote the conditional probability density of a first such encounter between t and $t + \mathrm{d}t$ as $r(t, d|r_0)$. As the interdiffusion coefficients of RP 1 and RP 2 might be different and the transformation of the pairs might remove or create a Coulombic interaction between the radicals, $r(t, d|r_0)$ need not be identical for RP 1 and RP 2. Furthermore, owing to the interconversion of the pairs, a pair starting out as RP 1 may reencounter as RP 1 or as RP 2. The four possible cases are distinguished by subscripts *ij* ($i, j = 1, 2$), where the second index denotes the chemical state of the pair at the beginning of the diffusional excursion, and the first index its state at the reencounter.

Averaging the elements of $\vec{\rho}$ over time with the respective weights $r_{ij}(t, d|r_0)$ yields an averaged density vector $\bar{\vec{\rho}}_{\mathrm{after}}$ that can be calculated from the density vector before the diffusional excursion, $\vec{\rho}_{\mathrm{before}}$, by

$$\vec{\rho}_{\mathrm{after}} = \hat{\mathrm{M}}\vec{\rho}_{\mathrm{before}}$$

$$\hat{\mathrm{M}} = {}^1/_2 \begin{pmatrix} f_{11} + g_{11} & f_{11} - g_{11} & p_{12} - \bar{f}_{12} + h_{12} & p_{12} - \bar{f}_{12} - h_{12} \\ f_{11} - g_{11} & f_{11} + g_{11} & p_{12} - \bar{f}_{12} - h_{12} & p_{12} - \bar{f}_{12} + h_{12} \\ p_{21} - f_{21} + \bar{h}_{21} & p_{21} - f_{21} - \bar{h}_{21} & \bar{f}_{22} + \bar{g}_{22} & \bar{f}_{22} - \bar{g}_{22} \\ p_{21} - f_{21} - \bar{h}_{21} & p_{21} - f_{21} + \bar{h}_{21} & \bar{f}_{22} - \bar{g}_{22} & \bar{f}_{22} + \bar{g}_{22} \end{pmatrix} \tag{21}$$

The elements of the matrix $\hat{\mathrm{M}}$ are the total probabilities of at least one reencounter

$$p_{ij} = \int_0^\infty r_{ij}(t, d|r_0)\,\mathrm{d}\,t \tag{22}$$

and the integrals over the terms *F* (eq 5), *G* (eq 13), and *H* (eq 14),

$$f_{ij} = \int_0^\infty F(k_{\mathrm{for}}, k_{\mathrm{bck}})\, r_{ij}(t, d|r_0)\,\mathrm{d}\,t \tag{23}$$

$$g_{ij} = \int_0^\infty G\,(k_{\mathrm{for}}, k_{\mathrm{bck}}; q_{\mathrm{l}}, q_2)\, r_{ij}(t, d|r_0)\,\mathrm{d}\,t \tag{24}$$

$$h_{ij} = \int_0^\infty H\,(k_{\mathrm{for}}, k_{\mathrm{bck}}; q_{\mathrm{l}}, q_2)\, r_{ij}(t, d|r_0)\,\mathrm{d}\,t \tag{25}$$

The overlined parameters $\bar{f}_{ij}$, $\bar{g}_{ij}$, and $\bar{h}_{ij}$ are obtained by interchanging k_{for} and k_{bck}, as well as q_{l} and q_2 in the respective integrand.

Finally, the contributions from all reencounters are summed up in the usual way[13] by using a geometric series of matrices. This leads to the quantities F^*_{11}, F^*_{12}, F^*_{21}, and F^*_{22} (eq 26). The meaning of the indices is the same as before. Hence, F^*_{11} and F^*_{12} give the yields of geminate products from pairs RP 1 for a singlet reactivity of unity of either pair, and with the system starting out from the triplet state of RP 1, or of RP 2, respectively. F^*_{21} and F^*_{22} are the corresponding yields from pairs RP 2.

$$F^*_{ij} = u_i\,[\hat{\mathrm{E}} - \hat{\mathrm{M}}\ \mathrm{diag}(0\ 1\ 0\ 1)]^{-1}\ v_j \qquad i,j = 1,2 \tag{26}$$

with

$$u_1 = (1\ 0\ 0\ 0) \qquad u_2 = (0\ 0\ 1\ 0)$$

$$v_1 = \begin{pmatrix}0\\1\\0\\0\end{pmatrix} \qquad v_2 = \begin{pmatrix}0\\0\\0\\1\end{pmatrix}$$

In eq 26, $\hat{\mathrm{E}}$ is the unit matrix, $\hat{\mathrm{M}}$ is given by eq 21, and the exponent -1 denotes matrix inversion. By inserting the matrix elements of $\hat{\mathrm{M}}$, one obtains

$$F^*_{11} = [(p_{12} - \bar{f}_{12} - h_{12})\,(p_{21} - f_{21} + \bar{h}_{21}) - (f_{11} - g_{11})\,(\bar{f}_{22} + \bar{g}_{22} - 2)]/N \tag{27}$$

$$F^*_{12} = 2[h_{12}(f_{11} - 1) - (p_{12} - \bar{f}_{12})\,(g_{11} - 1)]/N \tag{28}$$

$$F^*_{21} = 2[\bar{h}_{21}(\bar{f}_{22} - 1) - (p_{21} - f_{21})\,(\bar{g}_{22} - 1)]/N \tag{29}$$

$$F^*_{22} = [(p_{12} - \bar{f}_{12} + h_{12})\,(p_{21} - f_{21} - \bar{h}_{21}) - (\bar{f}_{22} - \bar{g}_{22})\,(f_{11} + g_{11} - 2)]/N \tag{30}$$

All these expressions have the same denominator N,

$$N = 4 + (f_{11} + g_{11})\,(\bar{f}_{22} + \bar{g}_{22} - 2) - (p_{12} - \bar{f}_{12} + h_{12})\,(p_{21} - \mathrm{f}_{21} + \bar{h}_{21}) \tag{31}$$

As shown in ref 13a, arbitrary initial populations of $|\mathrm{S}\rangle$ and $|\mathrm{T}_0\rangle$ and singlet reactivities different from unity can be treated in terms of two key parameters only. One is the spin-independent total reaction probability of singlets, including all reencounters, the other is the pertaining F^*. Hence, eqs 27−30 are of general applicability. In particular, they are valid for any diffusional model as long as the strong-exchange case is realized.

CIDNP net polarizations are finally obtained from the F^* by calculating these quantities for all nuclear spin states of a particular nucleus and summing up their differences over all its NMR transitions.

Solution for a Specific Diffusional Model. To obtain numerical results, a diffusional model must be chosen. Because for many of the parameters exact values are unavailable, and the functional forms of the conditional probability densities $r_{12}(t, d|\mathrm{r}_0)$ and $r_{21}(t, d|\mathrm{r}_0)$ are unknown, all four probability densities of reencounter were taken to be equal, and approximated by the Noyes function[17] $r(t, d|d)$,

$$r(t, d|d) = \frac{p(1-p)d}{\sqrt{4\pi D}}\,t^{-3/2}\,\exp\left[-\frac{(1-p)^2 d^2}{4Dt}\right] \tag{32}$$

where D is the interdiffusion coefficient. The model underlying eq 32 is diffusion by steps of length λ_D ($\lambda_\mathrm{D} < d$) in the absence of an attractive or repulsive interaction between the radicals. The total probability p of reencounter is approximately given by[18]

$$p \approx [1 + 2\lambda_\mathrm{D}/(3d)]^{-1} \tag{33}$$

In the Noyes model, the initial distance and the reencounter distance are identical. This is compatible with the treatment of the previous sections because in the strong exchange limit CIDNP is only generated during those segments of the diffusional trajectories that fall outside the exchange region d.

The use of eq 32 implies neglect of the Coulombic attraction that is present in RP 1 but not in RP 2. However, it is estimated that this will not lead to a significant error because our experiments are carried out in the highly polar solvent water. Furthermore, at the boundary of the exchange region the Coulombic potential is already shielded by a few solvent layers. The error resulting from replacing the "mixed" probability densities of reencounter $r_{12}(t, d|r_0)$ and $r_{21}(\mathrm{t}, d|r_0)$ by eq 32 must be even smaller because these functions describe situations where the radicals do not experience a Coulombic interaction during a considerable part of their diffusional excursions. Lastly, use of the same function for RP 1 and RP 2 is equivalent to assuming equal interdiffusion coefficients. As deprotonation and cyclization of the methionine radical cation leaves the volume occupied by the molecule almost unchanged, this is probably a very good approximation.

Calculating the time averages according to eqs 23−25 leads to

$$\vec{\rho}_{\mathrm{tot,\ Noyes}}(t) = \begin{pmatrix} f & p - \bar{f} \\ p - f & \bar{f} \end{pmatrix}\vec{\rho}_{\mathrm{tot}}(0) \tag{34}$$

where p is the total recombination probability (eq 33), and f is given by

$$f = \frac{p}{k_\mathrm{for} + k_\mathrm{bck}}\{k_\mathrm{for}\,\exp\,[-(1-p)\,\sqrt{(k_\mathrm{for} + k_\mathrm{bck})\,d^2/D}] + k_\mathrm{bck}\} \tag{35}$$

Interchanging the arguments k_for and k_bck in this expression yields $\bar{f}$.

Likewise,

$$\vec{\rho}_{\mathrm{diff,\ Noyes}}(t) = \begin{pmatrix} g & h \\ \bar{h} & \bar{g} \end{pmatrix}\vec{\rho}_{\mathrm{tot}}(0) \tag{36}$$

with

$$g = \frac{p}{2}\{\exp\,(-y_+)\,\cos\,(z_+)\,(1+\alpha) + \exp\,(-y_-)\,\cos\,(z_-)\,(1-\alpha) + [\mathrm{sign}\,(v_+)\,\exp\,(-y_+)\,\sin\,(z_+) - \mathrm{sign}\,(v_-)\,\exp\,(-y_-)\,\sin\,(z_-)]\,\beta\} \tag{37}$$

$$h = \frac{pk_\mathrm{bck}}{\mathrm{Re}^2\,w + \mathrm{Im}^2\,w}\{[\exp\,(-y_-)\,\cos\,(z_-) - \exp\,(-y_+)\,\cos\,(z_+)]\,\mathrm{Re}\,w + [\mathrm{sign}\,(v_+)\,\exp\,(-y_+)\,\sin\,(z_+) - \mathrm{sign}\,(v_-)\,\exp\,(-y_-)\,\sin\,(z_-)]\,(-\mathrm{Im}\,w)\} \tag{38}$$

$$y_{\pm} = (1-p)\sqrt{\frac{(\sqrt{u_{\pm}^2+v_{\pm}^2}+u_{\pm})\,d^2}{2D}} \quad (39)$$

$$z_{\pm} = (1-p)\sqrt{\frac{(\sqrt{u_{\pm}^2+v_{\pm}^2}-u_{\pm})\,d^2}{2D}} \quad (40)$$

where α, β, u_+, u_-, v_+, v_-, Re w, and Im w have been defined in eqs 15−20. The quantities $\bar{g}$ and $\bar{h}$ are obtained from the expression for g and h, respectively, by interchanging the rate constants k_{for} and k_{bck}, as well as the matrix elements of intersystem crossing q_1 and q_2 everywhere, that is, also in the coefficients α and β (eqs 15 and 16).

Because the same function is used for the four conditional probability densities of reencounter, the matrix $\hat{M}$ of eq 21 is transformed into a slightly simpler form, with all the indices omitted. The same holds for the expressions for F_{11}^* to F_{22}^* (eqs 27−30). As a further simplification, in this system CIDNP experiments cannot differentiate between F_{11}^* and F_{12}^* nor between F_{21}^* and F_{22}^* because establishment of the equilibrium between the geminate products of RP 1 and RP 2, H-Met and Met^-, is fast on the NMR time scale. Hence, one detects the sums

$$(F_{11}^* + F_{12}^*)_{Noyes} = \{f(\bar{g}+h) + (\bar{f}-2)(g+\bar{h}) + g\bar{g} - h\bar{h} + [2-(f+\bar{f})-(h-\bar{h})-2\bar{g}]\,p + p^2\}/n \quad (41)$$

$$(F_{21}^* + F_{22}^*)_{Noyes} = \{\bar{f}(g+\bar{h}) + (f-2)(\bar{g}+h) + g\bar{g} - h\bar{h} + [2-(f+\bar{f})-(h-\bar{h})-2g]\,p + p^2\}/n \quad (42)$$

with

$$n = 4-2[(f+\bar{f})+(g+\bar{g})] + f(\bar{g}+h) + \bar{f}(g+\bar{h}) + g\bar{g} - h\bar{h} + [(f+\bar{f})-(h+\bar{h})]\,p - p^2$$

Some further simplification is possible by noting that

$$f + \bar{f} = p\exp[-(1-p)\sqrt{(k_{for}+k_{bck})d^2/D}]$$

$$g + \bar{g} = p[\exp(-y_+)\cos(z_+) + \exp(-y_-)\cos(z_-)]$$

$$h \pm \bar{h} = h(1 \pm k_{for}/k_{bck})$$

Fit Results. In order to apply these formulas to the experimental data (Figure 2), magnetic and diffusional parameters of the radical pairs must be provided. The g value of $CB^{\bullet-}$ is approximated by the g value of the radical anion of benzophenone, 2.0037,[19a] the g values of the open-chain sulfur-centered radical cations H-$Met_{op}^{\bullet+}$ and $Met_{op}^{\bullet}$ are assumed to be identical to the g value of the dimeric (i.e., $S^{+}\therefore S$-bridged) radical cation of *N*-acetylmethionine, 2.009,[19b] and for $Met_{cy}^{\bullet}$ we take the g value in solid matrix, 2.005.[5b] In the open-chain radical cations, the hyperfine coupling constant of H^{α} is zero; that of H^{γ} is estimated to be 1.95 mT, again using the dimeric radical of *N*-acetylmethionine as a model compound but doubling the (average) value of the hyperfine coupling constants given in ref 19b to take into account that in our monomeric radical cations the spin density on sulfur is twice as high. For strong magnetic fields and large differences Δg CIDNP intensities are directly proportional to the hyperfine coupling constants,[1b] so the limiting polarization ratio at high pH fixes the ratio of hyperfine coupling constants of the α and γ protons in $Met_{cy}^{\bullet}$.[5e] By choosing the radical cation of *N*-methylpyrrolidone (average of the splittings of the methylene α protons 4.25 mT)[19c] as a model compound for a cyclic nitrogen-centered radical cation and applying McConnell-type relationships[19d] we find that in the two-center−three-electron bond about one third of the unpaired spin density is shifted from sulfur to nitrogen,[5e] and we arrive at hyperfine coupling constants of 1.43 mT and 1.30 mT for H^{α} and H^{γ} in the cyclic radical cation $Met_{cy}^{\bullet}$. An exchange volume d of 7 Å and an interdiffusion coefficient of 2×10^{-5} cm^2 s^{-1} were assumed. With this value of d and a length of 1.5 Å for a diffusional step, eq 33 predicts a total probability p of reencounter of about 0.9. All rate constants, not only those in the arguments of the exponential, cosine, and sine functions, were expressed in units of d^2/D.

No complications can arise from protonation of $CB^{\bullet-}$ to give a ketyl radical ($pK_a = 8.2$) in our experiments because this reaction is slower than the radical pair life by several orders of magnitude.[20]

A solution for CIDNP in a three-site exchange according to Chart 2 is not available and would also almost certainly be untractable in practice because the complexity of the expressions already rises steeply in going from a single irreversible reaction[4] to a reversible one. Nor is it to be expected that such a model would yield more information for the system under study, where the radical pairs containing H-$Met_{op}^{\bullet+}$ and those containing $Met_{op}^{\bullet}$ cannot be distinguished by CIDNP. Suitable simplifications must thus be introduced that allow a description of this system in terms of a two-site exchange.

We will first show that a good fit to the experimental data cannot be reached on the assumption that all protonation and deprotonation steps are slow on the CIDNP timescale, although this hypothesis would not appear unreasonable a priori. With this scenario, H-$Met_{op}^{\bullet+}$ remains unchanged during the lifetime of the radical pairs and only gives rise to polarizations of H_{γ}, while the cyclization equilibrium between $Met_{op}^{\bullet}$ and $Met_{cy}^{\bullet}$ leads to polarizations of both H^{α} and H^{γ}. The initial mole fractions of H-$Met_{op}^{\bullet+}$ and $Met_{op}^{\bullet}$ can be described by a pH-dependent preequilibrium. The associated pK value should in principle be equal to pK_{a2} of the starting amino acid, but for complete generality we omit this identification. With this model, the polarization ratio (P_{α}/P_{γ}) is given by

$$(P_{\alpha}/P_{\gamma}) = \frac{KP_{\alpha}(k_c, k_{-c}; \omega_1, \omega_2)}{[H^+]P_{\gamma}(0, 0; \omega_1, \omega_2) + KP_{\gamma}(k_c, k_{-c}; \omega_1, \omega_2)} \quad (43)$$

where $P_i(k, k'; \omega_1, \omega_2)$ is the exchange-dependent polarization of proton i, which can be calculated from the formulas derived in the preceding sections. In the argument of this expression, ω_1 and ω_2 refer to RP 1 and RP 2, respectively, k is the first-order rate constant for the transformation RP 1 → RP 2 and k' that of the reverse reaction. With the present model, RP 1 denotes the radical pair containing $Met_{op}^{\bullet}$ and RP 2 that containing $Met_{cy}^{\bullet}$; k_c and k_{-c} have been defined in Chart 2. When the ratios r_1 and r_2 are introduced,

$$r_1 = P_{\alpha}(k_c, k_{-c}; \omega_1, \omega_2)/P_{\gamma}(k_c, k_{-c}; \omega_1, \omega_2)$$

$$r_2 = P_{\gamma}(k_c, k_{-c}; \omega_1, \omega_2)/P_{\gamma}(0, 0; \omega_1, \omega_2)$$

Equation 43 is recognized as a titration curve with an apparent equilibrium constant K', $K' = Kr_2$,

$$(P_{\alpha}/P_{\gamma}) = \frac{K'}{[H^+]K'}r_1 \quad (44)$$

A one-parameter fit of eq 44 to the experimental data, with r_1 fixed to the limiting polarization ratio at high pH, gave a value of 8.96 for pK'. This best fit is shown in Figure 3. It is obvious that the fit curve does not reproduce the experimental polarization ratios well because the transition regime is too narrow. We stress that this result depends neither on the premise that K in eq 43 and K_{a2} of the starting amino acid are identical nor on any assumptions regarding the magnetic parameters; such assumptions would only be necessary to extract rate constants from the best fit values of pK' (or r_2) and r_1. When a two-parameter fit (variables pK' and r_1) is performed, the least-square deviation decreases slightly, but the high-pH limit of the fit curve becomes much too low.

Next, we allow for a reaction H-Met$^{\bullet+}_{op} \rightarrow$ Met$^{\bullet}_{cy}$ with a rate that is no longer slow on the CIDNP timescale. To retain a two-site exchange, one must then assume that the deprotonated open-chain radical Met$^{\bullet}_{op}$ rapidly reacts to Met$^{\bullet}_{cy}$ such that as far as CIDNP is concerned the system starts out with a mixture of H-Met$^{\bullet+}_{op}$ and Met$^{\bullet}_{cy}$ with mole fractions reflecting the protonation equilibrium of the educts. This is certainly not an implausible hypothesis for the following reasons. First, cyclization of Met$^{\bullet}_{op}$ is an intramolecular process and should thus have a high frequency factor. Second, from the experimental data[5c,5d] it seems likely that this step is also exergonic. Third, the intrinsic activation barrier of such a cyclization should be fairly low because the structural changes during formation of the two-center-three-electron bond are much smaller than, for instance, in deprotonation, where a full σ-bond must be broken and another one formed. While this model is valid for an irreversible reaction RP 1 $\rightarrow$ RP 2, it can also be extended, without increase of the complexity of the expressions, to cover a reversible two-site exchange RP 1 $\rightleftharpoons$ RP 2 with pH-independent rate constants k_{12} and k_{21} of the forward and back reactions. For the polarization ratio, one obtains

$$(P_\alpha/P_\gamma) = \frac{[H^+]P_\alpha(k_{12}, k_{21}; \omega_1, \omega_2) + K_{a2}P_\alpha(k_{21}, k_{12}; \omega_2, \omega_1)}{[H^+]P_\gamma(k_{12}, k_{21}; \omega_1, \omega_2) + K_{a2}P_\gamma(k_{21}, k_{12}; \omega_2, \omega_1)} \quad (45)$$

As indicated by the function arguments, the polarizations in this expression must be calculated once with the variables in normal order and once with RP 1 and RP 2 (i.e., k_{12} and k_{21} as well as ω_1 and ω_2) interchanged. By rearranging eq 45 and introducing the abbreviations

$$x_1 = \frac{P_\alpha(k_{12}, k_{2l}; \omega_1, \omega_2)}{P_\gamma(k_{12}, k_{2l}; \omega_1, \omega_2)}$$

$$x_2 = \frac{P_\alpha(k_{21}, k_{12}; \omega_2, \omega_1)}{P_\gamma(k_{21}, k_{12}; \omega_2, \omega_1)}$$

$$x_3 = \frac{P_\gamma(k_{21}, k_{12}; \omega_2, \omega_1)}{P_\gamma(k_{12}, k_{2l}; \omega_1, \omega_2)}$$

$$K'' = K_{a2}x_3$$

one arrives at

$$(P_\alpha/P_\gamma) = \frac{[H^+]}{[H^+] + K''}x_1 + \frac{K''}{[H^+] + K''}x_2 \quad (46)$$

which shows that the polarization ratio is given by the superposition of the weighted titration curves for an acid and its conjugated base.

CHART 3

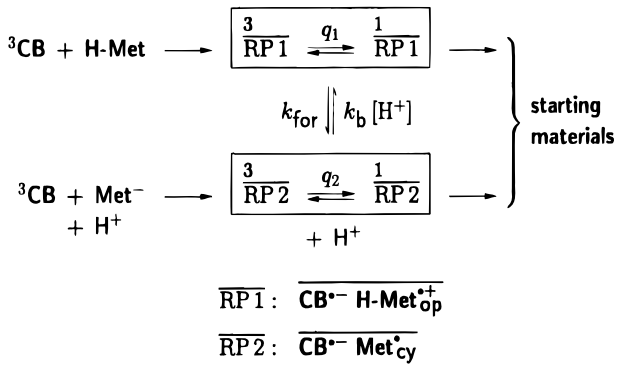

The best fit for such a model has also been included in Figure 3. It is evident that it does not represent the experimental data very well. Again, the deviations between the fit curve and the experimental curve are intrinsic to the model: Any contribution of the term $[H^+]/([H^+] + K'')$, which is unavoidable when the rate of the reaction RP 1 $\rightarrow$ RP 2 is nonnegligible, results in a residual floor of (P_α/P_γ) at low pH. This shows that a satisfactory explanation of the experimental polarization ratios is *impossible* by any two-site exchange model with *pH-independent* rate constants.

In contrast, a very good fit (see the figure) is obtained when the rate constant of the reverse reaction is taken to be proportional to $[H^+]$. Although this appears intuitively appealing, it must also be backed up by a derivation from the three-site exchange mechanism of Chart 2. However, such a model immediately follows when one assumes that in the sequence H-Met$^{\bullet+}_{op} \rightleftharpoons$ Met$^{\bullet}_{op} \rightleftharpoons$ Met$^{\bullet}_{cy}$ attainment of a steady state for the intermediate species Met$^{\bullet}_{op}$ is fast on the CIDNP time scale. This is not a very stringent condition but essentially a corollary to the hypothesis that cyclization of Met$^{\bullet}_{op}$ is fast on the CIDNP time scale, extensive numerical simulations indicating that after a time on the order of $5/k_c$ the concentration of Met$^{\bullet}_{op}$ deviates from the equilibrium concentration by less than 5%. When the steady-state approximation for Met$^{\bullet}_{op}$ is permissible, the problem can be formulated as a two-site exchange between H-Met$^{\bullet+}_{op}$ and Met$^{\bullet}_{cy}$ as shown in Chart 3. As before, the initial populations of the two radical species are determined by the protonation equilibrium of the starting amino acid, quenching of ^{3}CB by H-Met leading to H-Met$^{\bullet+}_{op}$, quenching by Met$^-$ directly (on the CIDNP time scale) to Met$^{\bullet}_{cy}$.

With this model, the apparent first-order rate constant k_{for} of the forward reaction is given by (for the definition of the microscopic rate constants, see Chart 2)

$$k_{for} = k_a + k'_a\frac{k_c}{k_c + k'_{-a}[H^+]}$$

Under the condition that $k_c \gg k'_{-a}[H^+]$, which is in accordance with the starting assumption of very fast cyclization, k_{for} becomes pH-independent,

$$k_{for} = k_a + k'_a \quad (47)$$

and the apparent first-order rate constant k_{bck} of the back reaction becomes proportional to $[H^+]$ and can be expressed as

$$k_{bck} = k_b[H^+] = k_{for}\frac{[H^+]}{K_a} \quad (48)$$

In contrast to the previous models, where the theory of pair substitution was not needed for fitting but only for interpretation of the best-fit parameters, with the present model this theory is a prerequisite of the fitting procedure because the terms P_i (k, k'; ω_1, ω_2) are now pH dependent, and thus different for each data point.

As Figure 3 shows, the data can be fitted almost perfectly in this way. This means that protonation/deprotonation at the radical pair stage significantly influences the CIDNP effects. Because k_{for} is a compound rate constant and also depends on the magnetic and diffusional parameters chosen, an unambiguous interpretation is not feasible on the basis of the existing information. The best-fit value of k_{for} is rather high (0.294 in units of d^2/D, corresponding to a rate constant of 1.2×10^9 s^{-1}); however, that k_{for} should be at least 1×10^8 s^{-1} can be inferred from the observation that in laser flash photolysis with optical detection on peptides with terminal methionine residues cyclization occurred even at pH well below pK_{a2} and was completed at the end of the laser flash (i.e., after 20 ns).[5d] Our fit furthermore gave a pK_a value of 8.15 for deprotonation of H-Met$^{\bullet+}_{op}$ with concomitant cyclization. This value is completely independent of the parameter d^2/D and only very weakly dependent on the magnetic parameters of the radical pairs.

On the basis of pK_a, the equilibrium constant K_c of cyclization (compare Chart 2) can be estimated in the following way. The shift of pK'_a from pK_{a2} (i.e., the difference of the acidities of the open-chain radical cation and the starting amino acid) is predominantly due to the positive charge attached to C^γ in H-Met$^{\bullet+}_{op}$. As a measure of this effect, we compare pK_{a1} and pK_{a2} of *N*-deuterated 1,3-diaminopropane.[21] The difference between these values is 1.15, after correcting for the statistical factors in this symmetrical diamine. The difference between pK_{a2} of methionine and pK_a of H-Met$^{\bullet+}_{op}$ in our system is larger by about 0.35 units. According to eq 1, this deviation must be ascribed to the cyclization, for which an equilibrium constant of 2.4 is obtained. While this value cannot be very accurate owing to the unavailability of suitable model compounds, it nevertheless indicates that cyclization is not strongly exergonic.

Experimental Section

Methionine, 4-carboxybenzophenone, and D_2O were obtained commercially in the highest purity available (>99%) and used as received. The concentration of the amino acid in the samples was 2×10^{-2} M and that of the sensitizer 2×10^{-3} M. The pH value was adjusted by addition of KOH and measured with a glass electrode. The solutions were deoxygenated by bubbling purified nitrogen through them, and the NMR tubes were then sealed.

The CIDNP experiments were performed on a Bruker WM-250 NMR spectrometer equipped with a home-made data acquisition system and pulser unit. As light source, an excimer laser (XeCl, $\lambda = 308$ nm) triggered by the pulse generator was used. The pulse sequences for the pseudo steady-state CIDNP measurements have been described previously.[22] This technique completely eliminates the background signals and yields CIDNP signals that are undistorted by nuclear spin relaxation in the diamagnetic reaction products. Ten laser flashes per acquistion were applied; for each spectrum, 16 transients were averaged. All measurements were carried out at room temperature.

Acknowledgment. This work was supported by the Volkswagenstiftung and the Committee of Scientific Research, Poland (Grant 2P303 049 06). J.R. thanks the DAAD for a scholarship. We are greatly indebted to Prof. Dr. U. Steiner, who stimulated this work by suggesting to us that the observed pH dependence of the polarization pattern might be a rate phenomenon.

References and Notes

(1) (a) Muus, L. T., Atkins, P. W., McLauchlan, K. A., Pedersen, J. B., Eds. *Chemically Induced Magnetic Polarization;* Reidel: Dordrecht, 1977. (b) Salikhov, K. M.; Molin, Yu. N.; Sagdeev, R. Z.; Buchachenko, A. L. *Spin Polarization and Magnetic Effects in Radical Reactions*; Elsevier: Amsterdam, 1984. (c) Goez, M. In *Advances in Photochemistry*; Neckers, D. C., Volman, D. H., von Bünau, G., Eds.; Wiley: New York, 1997; Vol. 23, pp 63−164.

(2) (a) Roth, H. D.; Manion, M. L. *J. Am. Chem. Soc.* **1975**, *97*, 6886−6888. (b) Roth, H. D. In Ref. 1a, pp 53−61.

(3) For example, see: (a) Roth, H. D. *Acc. Chem. Res.* **1987**, *20*, 343−350 and references therein. (b) Goez, M.; Rozwadowski, J.; Marciniak, B. *J. Am. Chem. Soc.* **1996**, *118*, 2882−2891.

(4) (a) Kaptein, R. *J. Am. Chem. Soc.* **1972**, *94*, 6262−6269. (b) Schwerzel, R. E.; Lawler, R. G.; Evans, G. T. *Chem. Phys. Lett.* **1974**, *29*, 106−109. (c) den Hollander, J. A. *Chem. Phys.* **1975**, *10*, 167−184. (d) den Hollander, J. A.; Kaptein, R. *Chem. Phys. Lett.* **1976**, *41*, 257−263. (e) Sarvarov, F. S.; Kobzareva, V. A.; Schmidt, V. N.; Salikhov, K. M. *Zh. Fiz. Khim.* **1982**, *56*, 1585−1597. (f) Hany, R.; Fischer, H. *Chem. Phys.* **1993**, *172*, 131−146.

(5) (a) Asmus, K.-D.; Göbl, M.; Hiller, K.-O.; Mahling, S.; Mönig, J. *J. Chem. Soc., Perkin Trans. 2* **1985**, 641−646. (b) Champagne, M. H.; Mullins, M. W.; Colson, A.-O.; Sevilla, M. D. *J. Phys. Chem.* **1991**, *95*, 6487−6493. (c) Bobrowski, K.; Hug, G. L.; Marciniak, B.; Kozubek, H. *J. Phys. Chem.* **1994**, *98*, 537−544. (d) Marciniak, B.; Hug, C. L.; Bobrowski, K.; Kozubek, H. *J. Phys. Chem.* **1995**, *99*, 13560−13568. (e) Goez, M.; Rozwadowski, J.; Marciniak, B. *Angew. Chem., Int. Ed. Engl.* **1998**, *37*, 628−630.

(6) (a) Prütz, W. A. In *Sulfur-Centered Reactive Intermediates in Chemistry and Biology*; Chatgilialoglu, C., Asmus, K.-D., Eds.; Plenum Press: New York, 1991; pp 389−399. (b) Schöneich, C.; Bobrowski, K.; Holcman, J.; Asmus, K.-D. In *Oxidative Damage and Repair. Chemical, Biological, and Medical Aspects;* Davies, K. E. J., Ed.; Pergamon Press: New York, 1991; pp 380−385.

(7) Another possible structure for the deprotonated radical cation of methionine is an adduct at sulfur with $^-$OH, a hydroxy sulfuranyl radical.[5a,c,d] By CIDNP, this species cannot be distinguished from the other open-chain radicals (see below, note 11), so we subsume it under Met$^{\bullet}_{op}$.

(8) Inbar, S.; Linshitz, H.; Cohen, S. G. *J. Am. Chem. Soc.* **1981**, *103*, 7323−7328.

(9) Gilbert, B. C. In *Sulfur-Centered Reactive Intermediates in Chemistry and Biology*; Chatgilialoglu, C., Asmus, K.-D., Eds.; Plenum Press: New York, 1991; pp 135−154.

(10) The hyperfine coupling constants of the protons at the nitrogen atom in Met$^{\bullet}_{cy}$ would be negative. However, because the amino protons exchange with the solvent D_2O, the nitrogen atoms bear only deuterons in our experiments.

(11) The *g* values of sulfuranyl radicals are identical to the *g* value of H-Met$^{\bullet+}_{op}$; the hyperfine coupling constants of the protons adjacent to sulfur are positive but somewhat smaller than those in the corresponding sulfur-centered radical cation.[9] The hyperfine coupling constant of the proton at the amino carbon in the hydroxy sulfuranyl radical must be negligible.

(12) Smith, R. M.; Martell, A. E. *Critical Stability Constants*; Plenum Press: New York, 1989; Vol. I, p 6.

(13) (a) Pedersen, J. B.; Freed, J. H. *J. Chem. Phys.* **1974**, *61*, 1517−1525. (b) Freed, J. H.; Pedersen, J. B. *Adv. Magn. Reson.* **1976**, *8*, 1−84. (c) Pedersen, J. B. *J. Chem. Phys.* **1977**, *67*, 4097−4102. (d) Pedersen, J. B. In Ref 1a, pp 297−308.

(14) Monchick, L.; Adrian, F. J. *J. Chem. Phys.* **1978**, *68*, 4372−4383.

(15) To simplify the following expressions, q_j has been chosen as twice the matrix element of intersystem crossing.

(16) Goez, M.; Heun, R. Unpublished results.

(17) Noyes, R. M. *J. Am. Chem. Soc.* **1956**, *78*, 5486−5490.

(18) Monchick, L. *J. Chem. Phys.* **1956**, *24*, 381−385.

(19) (a) Goez, M.; Sartorius, I. *J. Am. Chem. Soc.* **1993**, *115*, 11123−11133. (b) Naito, A.; Akasaka, K.; Hatano, H. *Mol. Phys.* **1981**, *44*, 427−443. (c) Eastland, R. W.; Rao, D. N. R.; Symons, M. C. R. *J. Chem. Soc., Perkin Trans. 2* **1984**, 1551−1557. (d) Carrington, A.; McLachlan, A. D. *Introduction to Magnetic Resonance*; Harper & Row: New York, 1969.

(20) Bobrowski, K.; Marciniak, B. *Radiat. Phys. Chem.* **1994**, *43*, 361−364.

(21) Jameson, R. F.; Hunter, G.; Kiss, T. *J. Chem. Soc. Perkin Trans. 2* **1980**, 1105−1110.

(22) Goez, M. *Chem. Phys. Letters* **1992**, *188*, 451−456.